International Journal of Heat and Mass Transfer 129 (2019) 1242–1249

Contents lists available at ScienceDirect

International Journal of Heat and Mass Transfer

journal homepage: www.elsevier.com/locate/ijhmt

Dual nature solution of water functionalized copper nanoparticles along a permeable shrinking cylinder: FDM approach

Feroz Ahmed Soomro [a], Aurang Zaib [c], Rizwan Ul Haq [b,*], M. Sheikholeslami [d]

[a] Department of Basic Sciences and Related Studies, Quaid-e-Awam University College of Engineering, Science and Technology, Larkana, Pakistan
[b] Department of Electrical Engineering, Bahria University, Islamabad, Pakistan
[c] Department of Mathematical Sciences, Federal Urdu University of Arts, Sciences & Technology, Gulshan-e-Iqbal, Karachi, Pakistan
[d] Department of Mechanical Engineering, Babol Noshiravni University of Technology, Babol, Iran

ARTICLE INFO

Article history:
Received 9 April 2018
Accepted 10 October 2018

Keywords:
Multiple solutions
Mixed convection flow
Slip effects
Nanofluid
Shrinking cylinder

ABSTRACT

Present framework is established to deal the characteristics of axisymmetric mixed convection flow with heat transfer of water based copper (*Cu*-water) nanofluid along a porous shrinking cylinder with slip effects. The physical problem is modeled in the form of set of partial differential equations (PDEs) including conservation of mass, momentum and energy equations along with defined boundary conditions. Such PDEs are adapted to ordinary differential equations (ODEs) by utilizing similarity transformation technique. System of equations is emerged with the expressions of nanoparticle and based fluid. Numerical solution of governing ODEs is sought by using Finite Difference Method (FDM) against the range of several pertinent physical parameters. Base fluid (water) is analyzed in the presence of nanoparticles. The model encounters buoyancy opposing and assisting flow regions. Present study reveals that the solution in the assisting flow region is unique whereas multiple solutions exist in the opposing flow region. The results also indicate the existence of multiple solutions for certain amount of mass suction parameter. Moreover, increase in slip parameters and nanoparticle volume fraction enhances the range of suction parameter where the similarity solutions exist. It is further found that due to increase of nanoparticle volume fraction the skin friction increases whereas heat transfer rate decreases.

1. Introduction

Since past few decades study of boundary layer flow along a shrinking cylinder has attained valuable attention for researchers due to its massive applications in industries and engineering processes. Major applications regarding stretching/shrinking sheet includes rubber sheets, glass fiber production, wire drawing, paper production, etc. The fluid flow over stretching cylinder was initially studied by Wang [1]. The study revealed that the similarity solutions do not exist for shrinking cylinder case. Later on, Ishak et al. [2] extended the work of Wang's problem by considering the suction/injection effects. In another study, Wang and Ng [3] considered the velocity-slip effects due to flow over stretching cylinder. The study concluded that slip greatly influence both fluid velocity and skin friction at the surface of the stretching cylinder. Ushak et al. [4] carried out numerical and analytical study of magnetohydrodynamic (MHD) flow and heat transfer over non-permeable horizontal stretching cylinder. Kumari and Nath [5] reported the study on the heat transfer and fluid flow characteristics over the vertical stretching cylinder. The cylinder was considered under partial heating and suction effects. Two types of temperature conditions, namely, variable heat temperature (VHT) and variable heat flux (VHF) revealed very useful results. The same problem was reconsidered for the horizontal stretching cylinder by Datta et al. [6]. Such physical phenomenon has applications in vast variety of fields, especially in nuclear reactors cooling process. Mukhopadhyay [7] taken into consideration the partial velocity-slip effects and prescribed surface temperature at the horizontal stretching cylinder exposed to the transverse magnetic field. Numerical solution as well as analytical solutions for special cases was reported in the study. Second-order velocity-slip and first-order thermal-slip effects due to flow of viscous incompressible fluid over a vertical shrinking cylinder were analyzed by Mishra and Singh [8].

Water, engine oil, glycol are the conventional fluids which are believed to have comparatively low thermal conductivity, hence are insufficient to meet the necessity of today's cooling rate. A dependable method to improve the thermal conductivity is to

* Corresponding author.
E-mail addresses: ideal_riz@hotmail.com, r.haq.qau@gmail.com (Rizwan Ul Haq).

https://doi.org/10.1016/j.ijheatmasstransfer.2018.10.051
0017-9310/

add nanoparticle in the base fluid. There are various kinds of nanofluid applications in nanotechnology for instance: electronics applications, transportation, cooling process in industry and nuclear reactors, drug delivery, miniature technology, etc. The word nanofluid was introduced by Choi [9]. Nanofluid is a suspension of a nanometer sized particles of oxides, metals, carbides, nitrides, or nanotubes in regular base fluids such as ethylene glycol, water, engine oil, etc. Experimental and numerical study has revealed that the thermal conductivity of nanofluid is significantly increased as compared to that of base fluids [10]. Nanofluid flow over the horizontal linear stretching sheet subject to the convective boundary conditions was studied by Mankinde and Aziz [11]. The numerical results were reported which depicts that nanofluid parameters greatly influence the flow characteristics. The problem was revisited by Mustafa et al. [12] by considering the normal stagnation-point flow over linear stretching sheet with constant surface temperature. The semi-analytic solutions were reported in the study. Furthermore, non-stagnant nanofluid flow due to stretching of nonlinear horizontal stretching sheet was studied by Rana and Bhargava [13]. Study of three types of nanofluids, namely, Cu, Al_2O_3 and TiO_2 merged with base fluid water was done by Hady et al. [14]. The flow of such fluids was considered over the nonlinear stretching sheet with variable surface temperature. Moreover, considered stretching surface was under the effects of thermal radiation. The numerical study depicts that among three nanofluids, TiO_2 -water shown higher cooling performance. Noghrehbadi et al. [15] performed numerical experiment on the MHD nanofluid flow over permeable stretching cylinder using Buongiorno's nanofluid model. Stagnation-point flow of Cu-water nanofluid over horizontal and exponential stretching cylinder with heat generation/absorption was taken into consideration by Sulochana and Naramgiri [16]. Shehzad et al. [17] considered the stagnation-flow of MHD nanofluid over stretching surface. The surface was considered subject to convective heat and mass transfer condition. The semi-analytic solutions using Homotopy Analysis Method was reported. Naramgiri and Sulochana [18] reported the study of MHD nanofluid flow over exponential stretching sheet. Flow was considered through porous medium. Thermal radiation and heat generation/absorption effects were incorporated. The study concluded that the heat and mass transfer effects are enhanced by the exponential parameter.

The no-slip condition is insufficient when the fluid has particular matter like suspensions, foams, polymer solutions and emulsions and many more. Flows inside internal cavities and polishing of artificial hearts are among many applications of slip flows. Turkyilmazoglu [19] considered the partial slip flow of viscoelastic fluid over stretching surface with constant and variable temperature. Wang [20] investigated the flow of viscous fluid over stretching sheet subject to partial slip condition and suction. In other paper, he [21] studied the flow over cylinder subject to partial slip. Analytical study on the MHD fluid flow over stretching surface with partial slip was carried out by Fang et al. [22]. Later on, the problem was revisited by including the second-order slip condition [23]. Uddin et al. [24] considered the flow of non-Newtonian nanofluid over permeable stretching surface under the effect of velocity slip. Recent study related to the dual nature solution of various kind of fluid models along different geometries are presented by various authors [25–29]

The close investigation of literature reveals that mixed convective flow of Cu-water nanofluid towards a permeable shrinking cylinder with slip effect has not been explored so far. The physical problem is modeled into mathematical form which contains governing equations: continuity, momentum and energy equation. Such equations are nonlinear coupled partial differential equations. Similarity transformation procedure is applied on such set of equations to change them into ordinary differential equations. Finally, the numerical solution is obtained utilizing Finite Difference Method.

2. Materials and methods

Consider the mixed convection Cu-water nanofluid flow and heat transfer along permeable shrinking cylinder which is shrinked from both directions with equal velocity $u_w(x) = ax/L$, where a is the arbitrary parameter and L is the characteristic length. The temperature at the shrinking cylinder is considered of the form $T_w(x) = T_\infty + bx/L$, where T_∞ represents the ambient fluid temperature. Moreover, velocity-slip of first-order is also utilized to better understand the performance of working nanofluid on characteristics of flow and heat transfer. See Fig. 1 for pictorial representation of the considered physical model. Applying Boussinesq approximations and under the considered assumptions, the governing equations may be written as:

$$\frac{\partial(ru)}{\partial x} + \frac{\partial(rv)}{\partial r} = 0 \tag{1}$$

$$u\frac{\partial u}{\partial x} + v\frac{\partial u}{\partial r} = \frac{\mu_{nf}}{\rho_{nf}}\left(\frac{\partial^2 u}{\partial r^2} + \frac{1}{r}\frac{\partial u}{\partial r}\right) + \frac{(\rho\beta)_{nf}}{\rho_{nf}}g(T - T_\infty) \tag{2}$$

$$u\frac{\partial T}{\partial x} + v\frac{\partial T}{\partial r} = \frac{k_{nf}}{(\rho c_p)_{nf}}\left(\frac{\partial^2 T}{\partial r^2} + \frac{1}{r}\frac{\partial T}{\partial r}\right) \tag{3}$$

subject to the boundary conditions:

$$\begin{aligned} &u = -u_w + a_1\frac{\partial u}{\partial r}, v = -V_w, T = T_w(x) + c_1\frac{\partial T}{\partial r} \text{ at } r = R, \\ &u \to 0, T \to T_\infty \text{ as } r \to \infty. \end{aligned} \tag{4}$$

where r is the radial coordinate, u is the velocity component in the $x-axis$ direction and v is the velocity component in the radial $r-axis$ direction, T_∞ is the ambient fluid temperature, T is the boundary layer fluid temperature, a_1 and c_1 are the arbitrary constants and g represents the gravitational acceleration. Nanofluid parameters are: nanoparticle volume fraction ϕ, dynamic viscosity μ_{nf}, density ρ_{nf}, thermal expansion coefficient β_{nf}, thermal conductivity k_{nf} and specific heat capacity $(\rho c_p)_{nf}$. Well define the property of nanoparticle solid fractions and base fluid by notations $(*)_s$ and $(*)_f$, respectively. The empirical relationships between them are given by [30]:

$$\left.\begin{aligned} &\mu_{nf} = \frac{\mu_f}{(1-\phi)^{2.5}}, \\ &\rho_{nf} = (1-\phi)\rho_f + \phi\rho_s, \\ &(\rho c_p)_{nf} = (1-\phi)(\rho c_p)_f + \phi(\rho c_p)_s, \\ &\frac{k_{nf}}{k_f} = \frac{(k_s+2k_f)-2\phi(k_f-k_s)}{(k_s+2k_f)+\phi(k_f-k_s)}. \end{aligned}\right\} \tag{5}$$

Note that considered working fluid is Cu-water nanofluid. Corresponding physical properties are given in Table 2.To nondimensionalize the governing Eqs. (1)–(4), we introduce the following similarity transformation:

$$f(\eta) = \frac{\psi}{xR\sqrt{\frac{av_f}{L}}}, \quad \theta(\eta) = \frac{T - T_\infty}{T_w - T_\infty}, \quad \eta = \frac{r^2 - R^2}{2R}\sqrt{\frac{a}{Lv_f}} \tag{6}$$

where η and v_f are the similarity variable and kinematic viscosity, respectively. ψ denotes the stream function which is defined as:

$$u = \frac{1}{r}\frac{\partial\psi}{\partial r}, \quad v = -\frac{1}{r}\frac{\partial\psi}{\partial x}. \tag{7}$$

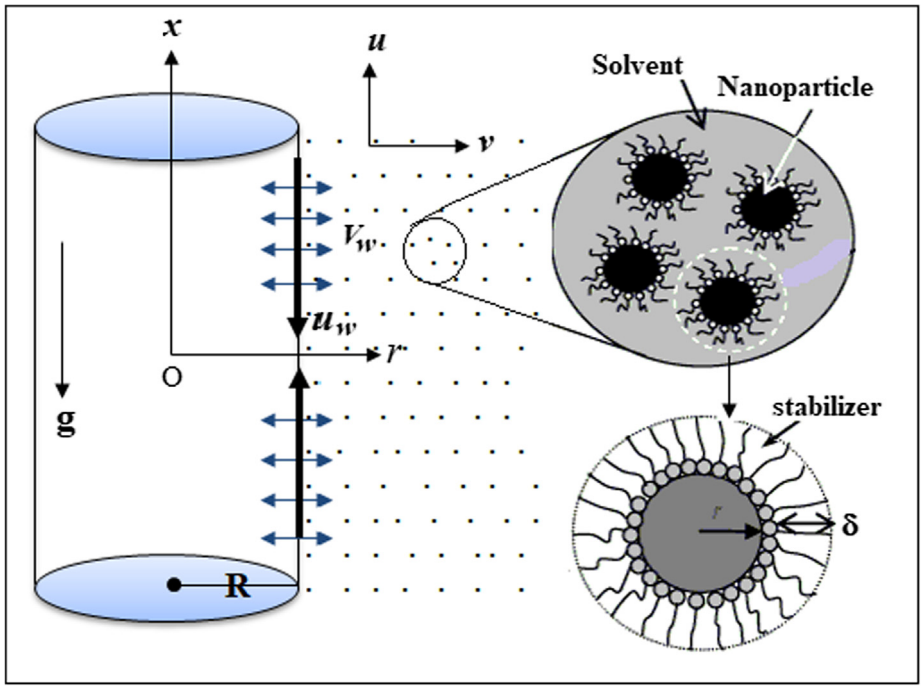

Fig. 1. The physical model of the problem.

Utilizing definition of stream functions (7) and (6) the governing Eqs. (1)–(3) along with boundary conditions (4) now may be written in nondimensional form as:

$$\frac{1}{(1-\phi)^{2.5}\left(1-\phi+\phi\frac{\rho_s}{\rho_f}\right)}\left[(1+2\gamma\eta)f'''+2\gamma f''\right]+ff''-f'^2 + \lambda\left(\frac{1-\phi+\phi\frac{(\rho\beta)_s}{(\rho\beta)_f}}{1-\phi+\phi\frac{\rho_s}{\rho_f}}\right)\theta=0 \tag{8}$$

$$\frac{k_{nf}}{k_f}\left[(1+2\gamma\eta)\theta''+2\gamma\theta'\right]+Pr\left[1-\phi+\phi\frac{(\rho c_p)_s}{(\rho c_p)_f}\right]\{f\theta'-f'\theta\}=0 \tag{9}$$

subject to the boundary conditions:

$$\left.\begin{aligned} &f(\eta)=S,\quad f'(\eta)=-1+\delta f''(\eta),\quad \theta(\eta)=1+\beta\theta'(\eta)\ \text{at}\ \eta=0\\ &f'(\eta)=0,\quad \theta(\eta)=0\ \text{as}\ \eta\to\infty \end{aligned}\right\} \tag{10}$$

In above set of equations and onwards prime notation denotes the ordinary differentiation with respect to similarity variable η and the emerging physical parameters are defined as:$\gamma=\sqrt{L\nu_f/aR^2}$ = curvature parameter, $\lambda=g\beta_f b/a^2$ = mixed convection parameter, $Pr=\nu_f/\alpha_f$ = Prandtl number, $\delta=a_1\sqrt{a/L\nu_f}$ = velocity slip parameter, $\beta=c_1\sqrt{a/L\nu_f}$ = thermal slip parameter, $S=V_w\sqrt{L/a\nu_f}>0$ = suction parameter.

Other than nanofluid velocity and temperature distribution the other quantities of interest are the wall drag and heat transfer which are denoted by coefficient of skin friction and Nusselt number, respectively, and are given by the following nondimensional expressions:

$$C_f=\frac{1}{(1-\phi)^{2.5}}f''(0)\ \text{and}\ Nu=-\frac{k_{nf}}{k_f}\theta'(0) \tag{11}$$

3. Results and discussion

3.1. Method and results validation

Numerical experiment is performed over the Eqs. (8)–(10) using numerical method called Finite Difference Method. By dropping few physical parameters our model reduces to the model already exists in the literature which shows that our model is more general. All the thermophysical properties of base fluid and nanoparticles are defined in Table 1. Though numerical results Table 2 provides the comparison of previously reported results [23] and present results. Two results are same which supports the validity of present model and obtained solutions.

Table 1
Thermophysical properties of fluid and nanoparticles.

Physical properties	Fluid phase (water)	Copper (*Cu*)
C_p (J/kg K)	4179	385
ρ (kg/m^3)	997.1	8933
k (W/mK)	0.613	400
$\alpha\times10^{-7}$ (m^2/s)	1.47	1163.1
$\beta\times10^{-5}$ (1/K)	21	1.67

Table 2
Comparison of $f''(0)$ with the existing work when $\lambda=0.5$, $\beta=\gamma=\phi=0$ and $S=2$.

Fang et al. [23] First solution		Present study First solution	
$\delta=-1.0$	$\delta=-2.0$	$\delta=-1.0$	$\delta=-2.0$
0.341159	0.20377	0.34121	0.20382
Second solution		Second solution	
0.31590	0.26557	0.31589	0.26561

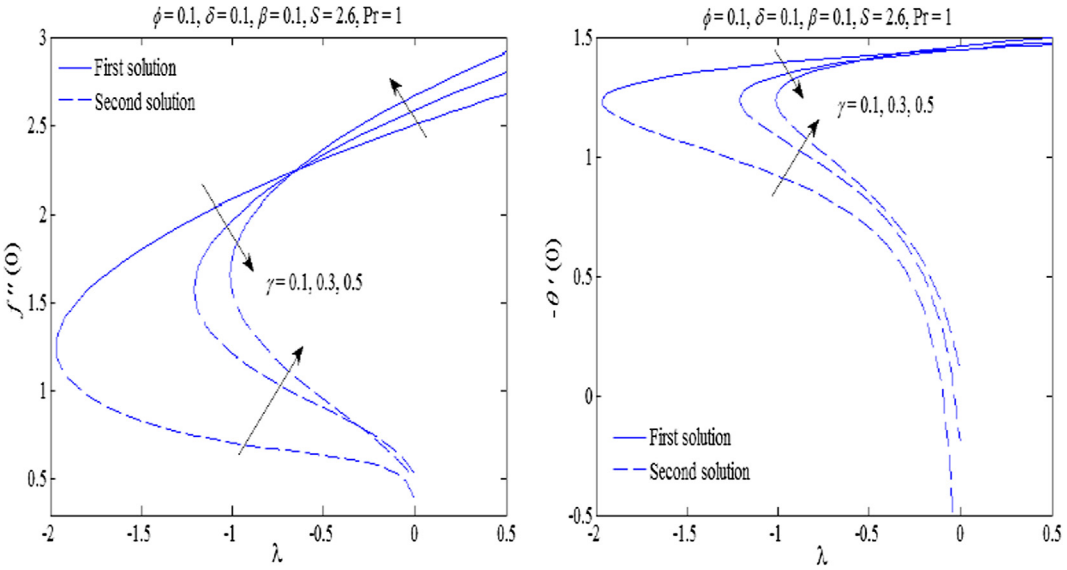

Fig. 2. Variation of (a) $f''(0)$ and (b) $-\theta'(0)$ against mixed convection parameter λ for different values of curvature parameter γ.

3.2. Variation of Nusselt number and skin friction coefficient

Fig. 2(a) and (b), respectively, shows the variation in coefficient of skin friction and Nusselt number due to variation in curvature parameter and buoyancy parameter. It can be see that dual solutions exist only for buoyancy opposing flow $\lambda < 0$ whereas solution is unique for buoyancy assisting flow $\lambda > 0$. Moreover, the solution does not exist for the values critical value buoyancy parameter λ say λ_c. Such values are computed as -1.8521, -1.0030 and -0.7300 for curvature parameter $\gamma = 0.1, 0.3, 0.5$, respectively. Fig. 2(a) shows that, for the second solution, the skin friction coefficient tends to increase. On the other hand, for the first solution, skin friction coefficient has different behavior for different range of buoyancy parameter.

It is observed that skin friction coefficient has different behavior in different range of curvature parameter. When $\lambda > -0.65$, the increase in curvature parameter enhances the coefficient of skin friction coefficient. On the other hand, when $\lambda < -0.65$, inverse trend of skin friction coefficient profiles are observed. Moreover, for the first solution, Nusselt number and curvature parameter in inversely proportional relation whereas for the second solution they are directly proportional. Overall, it is observed that due to increase value of buoyancy parameter the first solution tends to increase whereas second solution tends to decrease.

Fig. 3 presents the variations in Nusselt number and coefficient of skin friction against the increasing value of nanoparticle volume fraction and suction parameter. It is evident from the profile trend that, increase in nanoparticle volume fraction enhances the coefficient of skin friction and decreases the heat transfer rate. This fact is true for both first and second solution. Moreover, for the considered range of nanoparticle volume fraction, increase in suction parameter generates increase in coefficient of skin friction for the first solution and produces decrease for the second solution. On the other hand, increase in suction parameter produces increase

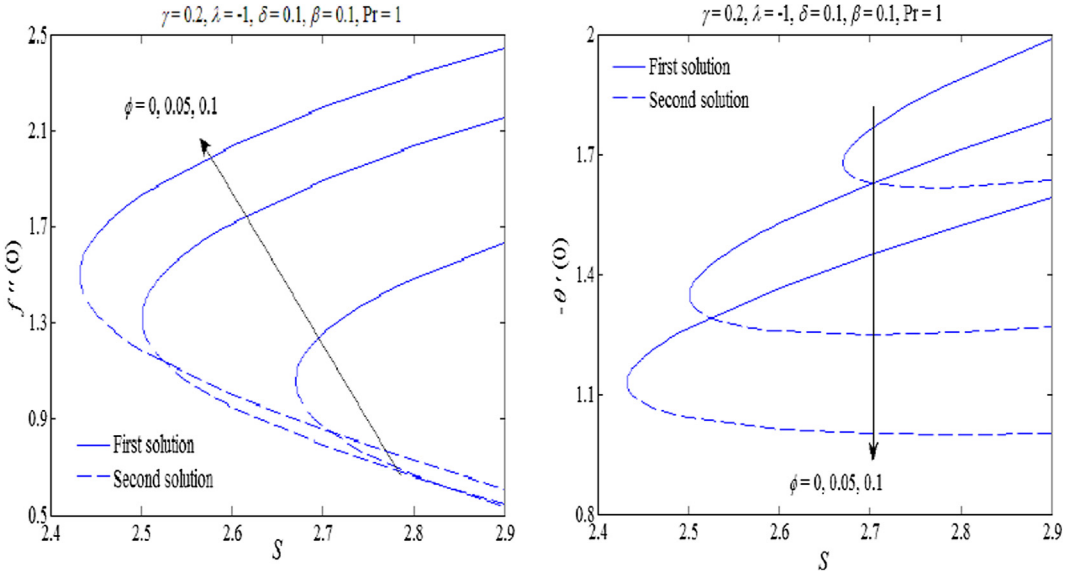

Fig. 3. Variation of (a) $f''(0)$ and (b) $-\theta'(0)$ against suction parameter S for different values of nanoparticle volume fraction ϕ.

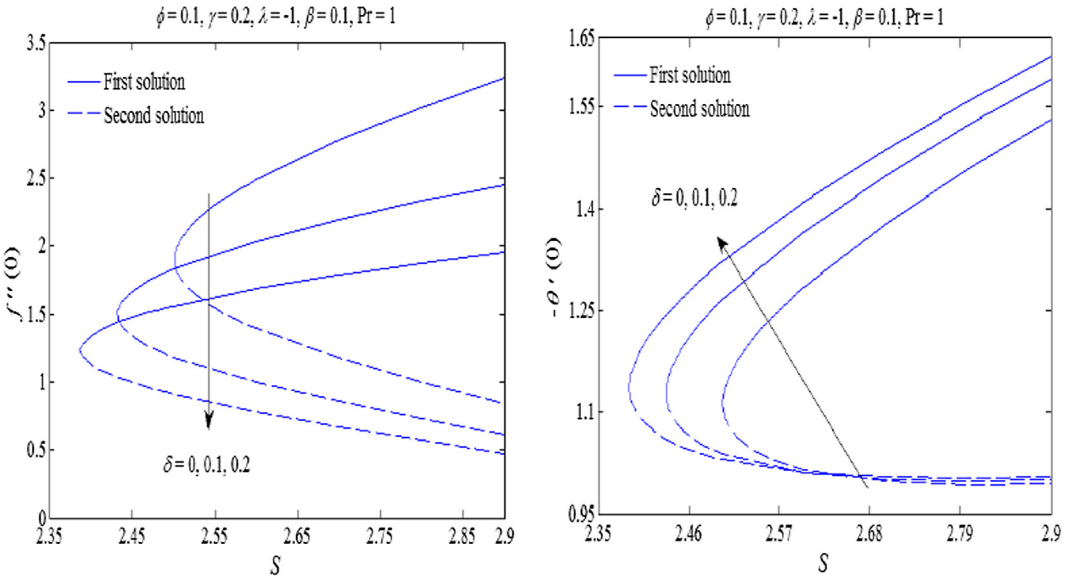

Fig. 4. Variation of (a) $f''(0)$ and (b) $-\theta'(0)$ against suctions parameter S for different values of velocity slip parameter δ.

in Nusselt number for the first solution whereas insignificant effect is observed for the second solution.

Variation in skin friction coefficient and Nusselt number due to suction and slip parameter is presented through Fig. 4(a) and (b), respectively. The trend of profiles shows that, for both first and second solution, skin friction coefficient is decreasing quantity and Nusselt number is increasing quantity of velocity slip parameter. On the other hand, suction parameter has different effects on the first and second solution. For the first solution, augmentation in Nusselt number and skin friction coefficient is observed due to increase suction parameter. For the second solution, increasing value of suction has decreasing effect on coefficient of skin friction whereas not significant effect has been noticed on the Nusselt number.

Fig. 5(a) and (b) shows the respective profile trends of skin friction coefficient and Nusselt number against the increasing value of suction and thermal slip parameters. It can be observed that, for the first solution, variation in coefficient of skin friction is directly proportional to the thermal slip and suction parameter whereas, for the second solution, inversely proportional behavior is observed. Moreover, Nusselt number and thermal slip parameter are inversely proportional for both first and second solutions. On the other hand, for the second solution, Nusselt number and suction parameter are directly proportional whereas not significant effect is observed for the second solution.

3.3. Variation of streamlines and isotherms

To analyze the effect of flow and heat transfer in the entire domain of the boundary layer, results are produce for stream function and Temperature that is define in the Eq. (6). One can see (Figs. 6 and 7) the stream lines exactly obey the flow behavior along a shrinking cylinder. Since fluid molecules follow the pattern of motion of the surface. Since surface of the cylinder is shrinking

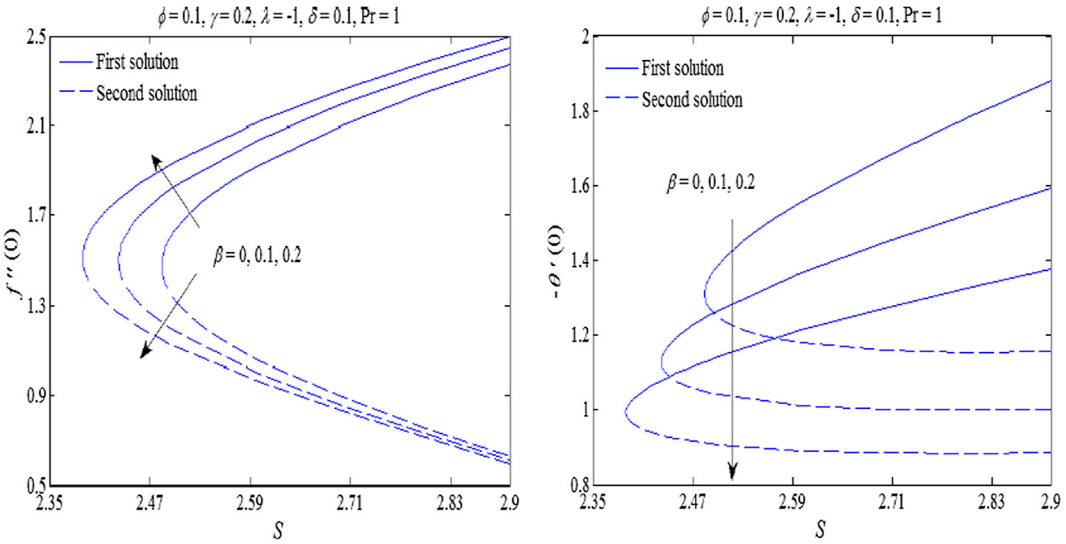

Fig. 5. Variation of (a) $f''(0)$ and (b) $-\theta'(0)$ against suction parameter S for different values of thermal slip parameter β.

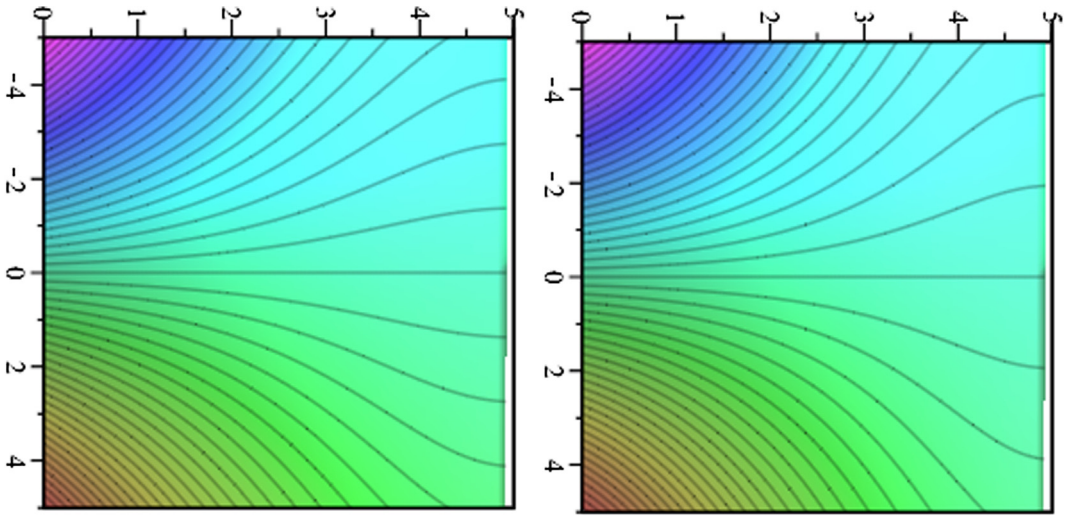

Fig. 6. Variation of stream lines for (a) $S = 0.5$ and (b) $S = 1$.

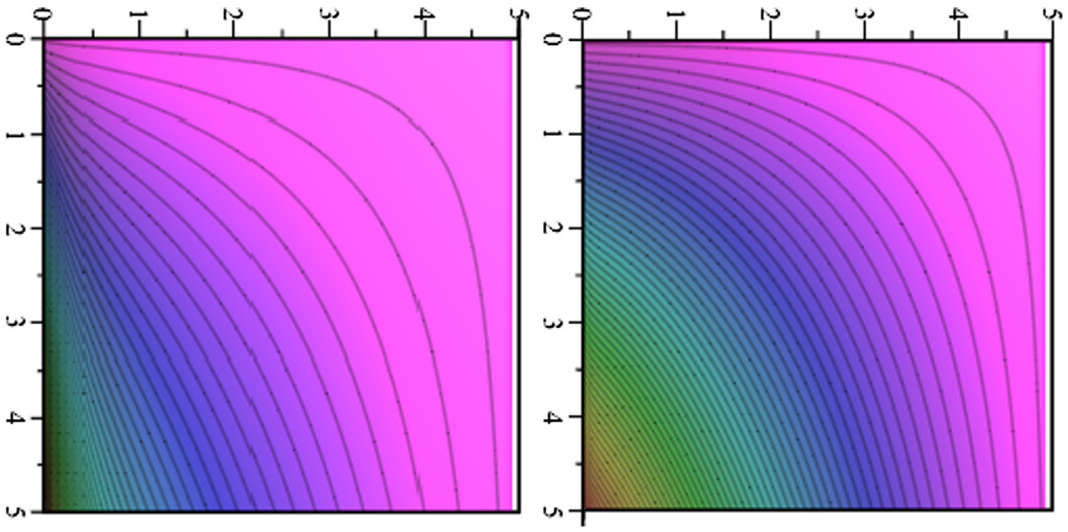

Fig. 7. Variation of isotherms for (a) $S = 0.5$ and (b) $S = 1$.

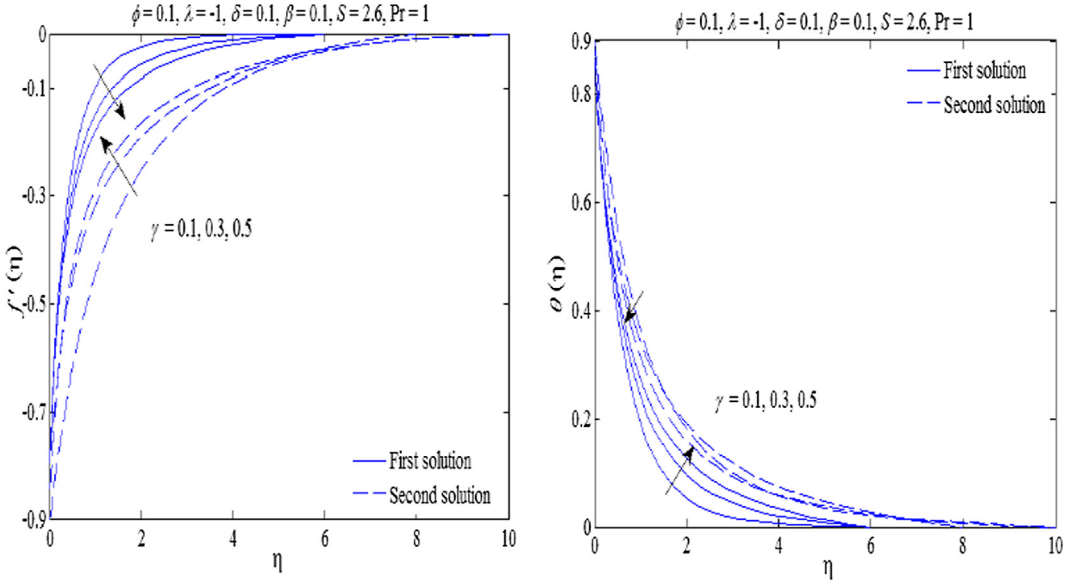

Fig. 8. The variation of (a) velocity $f'(\eta)$ and (b) temperature $\theta(\eta)$ profiles for different values of curvature parameter γ.

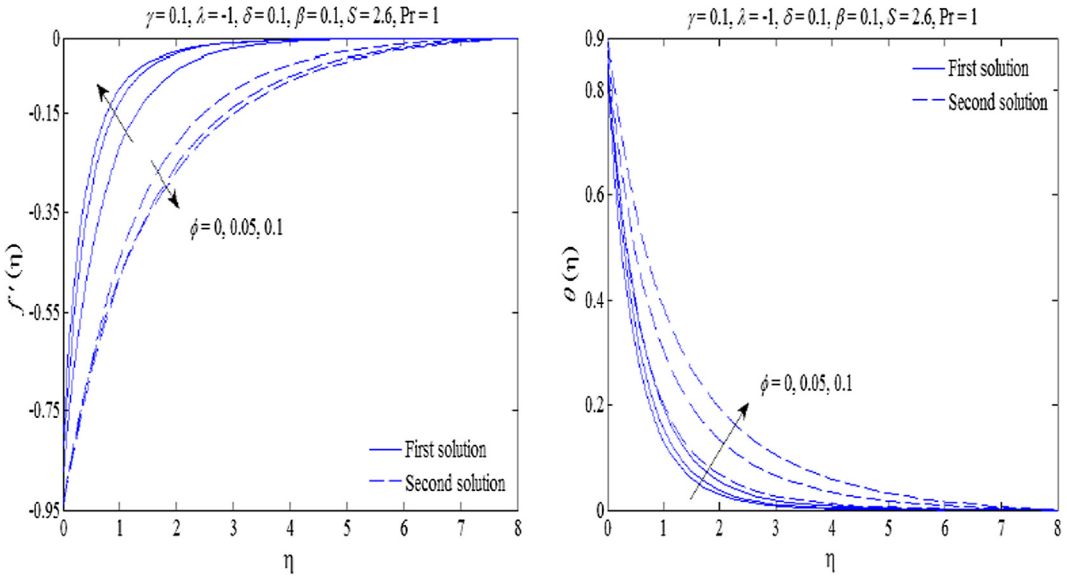

Fig. 9. The variation of (a) velocity $f'(\eta)$ and (b) temperature $\theta(\eta)$ profiles for different values of nanoparticle volume fraction ϕ.

Table 3
Values of $f''(0)$ and $-\theta'(0)$ against suction parameter S for some values of thermal slip parameter β when $\phi = 0.1, \gamma = 0.2, \lambda = -1, \delta = 0.2, Pr = 1$.

β	S	$f''(0)$	$-\theta'(0)$
0	2.5	1.6362	1.3862
		(1.3219)	(1.2491)
	2.6	1.9248	1.5550
		(1.0555)	(1.1805)
0.1	2.5	1.8318	1.2659
		(1.1832)	(1.0404)
	2.6	2.0382	1.3666
		(0.9991)	(1.0125)
0.2	2.5	1.9382	1.1417
		(1.1171)	(0.9071)
	2.6	2.1156	1.2126
		(0.9618)	(0.8912)

so fluid molecules are movies with respect to surface. Further it is analyzed that temperature of the surface of the cylinder is heated so one can observed that near the surface heat of the fluid is more dominant as compare to the away of the surface.

3.4. Variation of temperature and velocity profiles

Effect on the nanofluid velocity and temperature due to change in the curvature parameter γ is described through the Fig. 8(a) and (b), respectively. The profiles trends show the inverse effects for first and second solution. Curvature parameter increment, nanofluid velocity tends to decrease for the first solution, whereas it tends to increase for the second solution. On the other hand, nanofluid temperature is enhanced due to increase in curvature parameter for the first solution and decreasing profile trend is observed for the second solution. Furthermore, it is noticed that thermal and velocity boundary layer thickness is decreasing function of curvature parameter.

Change in nanofluid velocity and temperature due to change in nanoparticle volume fraction is presented through Fig. 9(a) and (b), respectively. For the first solution, nanofluid velocity is increased due to increment in nanoparticle volume fraction whereas inverse trend of profiles is observed for the second solution which shows that fluid velocity tends to decrease for the second solution. On the other hand, for both solutions, nanofluid temperature is increasing function of nanoparticle volume fraction. It can also be notified that increase in nanoparticle volume fraction has decreasing effect on thermal and velocity boundary layer thickness (see Table 3).

4. Conclusion

Numerical analysis on the flow and heat transfer characteristics of *Cu*-water nanofluid mixed convection flow towards the vertical permeable cylinder was done in contrast to the work of Mishra and Singh [31] in which conventional base fluid was utilized as a working fluid. In the absence of nanoparticles and second order slip parameter our model reduces to one already reported. So, present model is the generalization of the model presented by Mishra and Singh [31]. Apart from this studied our results are providing excellent comparison with the existing literature presented by Fang et al. [23] (see Table 2). The study revealed that dual nature of solutions exists for buoyancy opposing flow, while the solutions are unique for buoyancy assisting flow. The curvature parameter γ reduces the range of existence of the self similar solutions, which in turn accelerates the boundary layer separation. Shear stress is increased while the heat transfer rate is decreased due to increment in nanoparticle volume fraction. Moreover, the velocity slip parameter δ and thermal slip parameter β increases the range of suction parameter S for existence of self-similar solutions. However, for there is opposite trend can be found at skin friction due to increase in thermal slip parameter. It can be found that skin friction behavior increases for upper branch of the solution and decreases for lower branch of the solution. In similar manner, Nusselt number just depicts the decrease behavior for each nature of solution when thermal slip parameter increases.

Conflict of interest

There is no actual or potential conflict of interest including any financial, personal or other relationships with other people or organizations.

References

[1] C.Y. Wang, Fluid flow due to a stretching cylinder, Phys. Fluids 31 (3) (1988) 466–468.
[2] A. Ishak, R. Nazar, I. Pop, Uniform suction/blowing on flow and heat transfer due to a stretching cylinder, Appl. Math. Model. 32 (10) (2008) 2059–2066.
[3] C.Y. Wang, Chiu-On Ng, Slip flow due to a stretching cylinder, Int. J. Non Linear Mech. 46 (9) (2011) 1191–1194.
[4] A. Ishak, R. Nazar, I. Pop, Magnetohydrodynamic (MHD) flow and heat transfer due to a stretching cylinder, Energy Convers. Manage. 49 (11) (2008) 3265–3269.
[5] M. Kumari, G. Nath, Mixed convection boundary layer flow over a thin vertical cylinder with localized injection/suction and cooling/heating, Int. J. Heat Mass Transf. 47 (5) (2004) 969–976.
[6] P. Datta, D. Anilkumar, S. Roy, N.C. Mahanti, Effect of non-uniform slot injection (suction) on a forced flow over a slender cylinder, Int. J. Heat Mass Transf. 49 (13–14) (2006) 2366–2371.
[7] S. Mukhopadhyay, MHD boundary layer slip flow along a stretching cylinder, Ain Shams Eng. J. 4 (2) (2013) 317–324.
[8] U. Mishra, G. Singh, Dual solutions of mixed convection flow with momentum and thermal slip flow over a permeable shrinking cylinder, Comput. Fluids 93 (2014) 107–115.
[9] S. Choi, Enhancing thermal conductivity of fluids with nanoparticles, Develop. Appl. Non-Newtonian Flows 231 (1995) 99–105.
[10] P. Keblinski, J.A. Eastman, D.G. Cahill, Nanofluids for thermal transport, Mater. Today 8 (2005) 36–44.
[11] O.D. Makinde, A. Aziz, Boundary layer flow of a nanofluid past a stretching sheet with a convective boundary condition, Int. J. Therm. Sci. 50 (7) (2011) 1326–1332.
[12] M. Mustafa, T. Hayat, I. Pop, S. Asghar, S. Obaidat, Stagnation-point flow of nanofluid towards a stretching sheet, Int. J. Heat Mass Transf. 54 (25–26) (2011) 5588–5594.
[13] P. Rana, R. Bhargava, Flow and heat transfer of a nanofluid over a nonlinearly stretching sheet: a numerical study, Commun. Nonlinear Sci. Numer. Simul. 17 (1) (2012) 212–226.
[14] F.M. Hady, F.S. Ibrahim, S.M. Abdel-Gaied, M.R. Eid, Radiation effect on viscous flow of a nanofluid and heat transfer over a nonlinearly stretching sheet, Nanoscale Res. Lett. 7 (2012) 229–242.
[15] A. Noghrehabadi, M. Ghalambaz, E. Izadpanahi, R. Pourrajab, Effect of magnetic field on the boundary layer flow, heat, and mass transfer of nanofluids over a stretching cylinder, J. Heat Mass Transfer Res. 1 (1) (2014) 9–16.
[16] C. Sulochana, N. Naramgari, Stagnation point flow and heat transfer behavior of Cu-water nanofluid towards horizontal and exponentially stretching/shrinking cylinders, Appl. Nanosci. 6 (3) (2016) 451–459.
[17] S.A. Shehzad, T. Hayat, A. Alsaedi, Influence of convective heat and mass conditions in MHD flow of nanofluid, Bull. Polish Acad. Sci. Tech. Sci. 63 (2) (2015) 465–474.
[18] S. Naramgari, C. Sulochana, Dual solutions of radiative MHD nanofluid flow over an exponentially stretching sheet with heat generation/absorption, Appl. Nanosci. 6 (1) (2016) 131–139.
[19] M. Turkyilmazoglu, Multiple analytic solutions of heat and mass transfer of magnetohydrodynamic slip flow for two types of viscoelastic fluids over a stretching surface, ASME J. Heat Transfer 134 (7) (2012) e071701–e71711.
[20] C.Y. Wang, Analysis of viscous flow due to a stretching sheet with surface slip and suction, Nonlin. Anal. Real World Appl. 10 (1) (2009) 375–380.
[21] C.Y. Wang, Stagnation flow on a cylinder with partial slip - an exact solution of the Navier-Stokes equations, IMA J. Appl. Math. 72 (3) (2007) 271–277.
[22] T. Fang, J. Zhong, S. Yao, Slip MHD viscous flow over a stretching sheet – an exact solution, Commun. Nonlin. Sci. Numer. Simul. 14 (11) (2009) 3731–3737.
[23] T. Fang, S. Yao, J. Zhang, A. Aziz, Viscous flow over a shrinking sheet with a second order slip flow model, Commun. Nonlin. Sci. Num. Simul. 15 (7) (2010) 1831–1842.
[24] M.J. Uddin, M. Ferdows, O.A. Beg, Group analysis and numerical computation of magneto-convective non-Newtonian nanofluid slip flow from a permeable stretching sheet, Appl. Nanosci. 4 (7) (2014) 897–910.
[25] Hashim, M. Khan, A revised model to analyze the heat and mass transfer mechanisms in the flow of Carreau nanofluids, Int. J. Heat Mass Transf. 103 (2016) 291–297.
[26] Hashim, M. Khan, Critical values in flow patterns of Magneto-Carreau fluid over a circular cylinder with diffusion species: multiple solutions, J. Taiwan Inst. Chem. Eng. 77 (2017) 282–292.
[27] M. Khan, Hashim, A. Hafeez, A review on slip-flow and heat transfer performance of nanofluids from a permeable shrinking surface with thermal radiation: dual solutions, Chem. Eng. Sci. 173 (2017) 1–11.
[28] Hashim, M. Khan, A.S. Alshomrani, Numerical simulation for flow and heat transfer to Carreau fluid with magnetic field effect: dual nature study, J. Magn. Magn. Mater. 443 (2017) 13–21.
[29] Hashim, M. Khan, S.A. Alshomrani, Characteristics of melting heat transfer during flow of Carreau fluid induced by a stretching cylinder, Eur. Phys. J. E 40 (1) (2017).
[30] R.K. Tiwari, M.K. Das, Heat transfer augmentation in a two-sided lid-driven differentially heated square cavity utilizing nanofluids, Int. J. Heat Mass Transf. 50 (9–10) (2007) 2002–2018.
[31] U. Mishra, G. Singh, Dual solutions of mixed convection flow with momentum and thermal slip flow over a permeable shrinking cylinder, Comput. Fluids 93 (2014) 107–115.